Cancer photothermal therapy in the near-infrared region by using single-walled carbon nanotubes

Feifan Zhou
Da Xing
Zhongmin Ou
Baoyan Wu
South China Normal University
MOE Key Laboratory of Laser Life Science & Institute of Laser Life Science
Guangzhou 510631, China

Daniel E. Resasco
University of Oklahoma
School of Chemical, Biological and Materials Engineering
100 E Boyd Street
Norman, Oklahoma 73019

Wei R. Chen
South China Normal University
MOE Key Laboratory of Laser Life Science & Institute of Laser Life Science
Guangzhou 510631, China
and
University of Central Oklahoma
College of Mathematics and Science
Department of Engineering and Physics
Biomedical Engineering Program
Edmond, Oklahoma 73034

Abstract. Single-walled carbon nanotubes (SWNTs) have a high optical absorbance in the near-infrared (NIR) region. In this special optical window, biological systems are known to be highly transparent. The optical properties of SWNTs provide an opportunity for selective photothermal therapy for cancer treatment. Specifically, CoMoCAT® nanotubes with a uniform size (about 0.81 nm) and a narrow absorption peak at 980 nm are ideal candidates for such a novel approach. Here, CoMoCAT® SWNTs are conjugated to folate, which can bind specifically to the surface of the folate receptor tumor markers. Folate-SWNT (FA-SWNT) targeted tumor cells were irradiated by a 980-nm laser. In our *in vitro* and *in vivo* experiments, FA-SWNT effectively enhanced the photothermal destruction on tumor cells and noticeably spared the photothermal destruction for nontargeted normal cells. Thus, SWNTs, combined with suitable tumor markers, can be used as novel nanomaterials for selective photothermal therapy for cancer treatment.
[DOI: 10.1117/1.3078803]

Keywords: Near-infarred region; CoMoCAT nanotubes; photothermal therapy; floate single-walled carbon nanotubes.

Paper 08233SSR received Jul. 14, 2008; revised manuscript received Sep. 11, 2008; accepted for publication Sep. 11, 2008; published online Mar. 4, 2009.

1 Introduction

Photothermal therapies for cancer have been widely investigated as a minimally invasive treatment modality in comparison with other methods.[1–3] However, the chromophores in healthy tissue in the light path can also absorb energy, thus reducing the effectiveness of the heat deposition within tumor cells and increasing nonspecific injury of adjacent healthy tissue. *In situ* light-absorbing dyes have been used to selectively increase the thermal destructions in the target tumors.[4,5] Recently, nanotechnology has engendered a range of novel materials, such as gold nanoshells[6–8] and carbon nanotubes,[9,10] with unique optical properties such as a strong near-infrared absorption efficiency and photo-stability compared to the conventional dyes.

Single-walled carbon nanotubes (SWNTs) have been considered for applications in various biological systems, including deliveries of biological cargoes into cells, biosensor development, bioelectrochemistry, and biomedical devices.[11–15] The intrinsic property of SWNTs is their strong optical absorbance in the near-infrared (NIR) region,[9,16] which could release significant heat and enhance thermal destruction of cells during NIR laser irradiation[9] and radiofrequency irradiation.[17]

Address all correspondence to: Da Xing, MOE Key Laboratory of Laser Life Science & Institute of Laser Life Science, South China Normal University, Guangzhou 510631, China. Tel: +86-20-85210089; Fax: +86-20-85216052; E-mail: xingda@scnu.edu.cn

Since biological tissues exhibit a deep penetrability with very low absorption of NIR photons in the wavelength range of 700 to 1100 nm,[18,19] the SWNTs, with an absorption band in the NIR region, could be the ideal candidate for photothermal therapy.

The CoMoCAT® method[20] produces SWNTs that are enriched in the (6,5) nanotube chirality with a narrow and intense absorption band at 980 nm that has a uniform size of about 0.81 nm.[10] Its photothermal properties should be explored for selective photo-tissue interactions. Furthermore, photothermal therapy using the absorption properties of antibody-conjugated nanomaterials has demonstrated selective killing of cancer cells while leaving healthy cells unaffected.[6,9,21–23] In this study, we explored the effects of irradiation by a 980-nm laser of antibody-conjugated CoMoCAT® nanotubes, that can act efficiently to convert the 980-nm laser energy into heat and to selectively destroy target cells. We used a synthetic method to enable the conjugation of the SWNTs to folate moiety, which selectively internalized SWNTs inside cells labeled with folate receptor (FR) tumor markers.[9] In this paper, we present the results of cell death induced by the irradiation of a 980-nm laser, either *in vitro* or *in vivo* and with or without folate-SWNT (FA-SWNT).

1083-3668/2009/14(2)/021009/7/$25.00 © 2009 SPIE

2 Materials and Methods

2.1 *Chemicals and Plasmids*

The following chemicals and fluorophore probes were used: PL-PEG-NH_2 (Avanti Polar Lipids, Mt. Eden, AL), folate (Sigma, St. Louis, MO), fluoroscein isothiocyanate (FITC, Sigma), cell-counting kit 8 (CCK8, Dojindo Laboratories, Kumamoto, Japan), and an *in situ* cell death detection kit (TUNEL) (R&D Systems, Minneapolis, MN).

2.2 *CoMoCAT® Single-Walled Carbon Nanotubes*

The CoMoCAT® method produces single-walled carbon nanotubes using a silica-supported bimetallic cobalt-molybdate catalyst.[20] The material is composed of a narrow distribution of nanotube types, with the (6,5) semiconducting chirality dominating and an average diameter of 0.81 nm.[10] This type of nanotube possesses an intense absorption band at approximately 980 nm.[10]

2.3 *Absorption Spectra of the SWNT Suspension*

The absorption spectra of SWNT suspension were obtained using an ultraviolet-visible (UV/VIS) spectrometer (Lambda 35, Perkin-Elmer, USA), with a 2-nm slit width at a scan speed of 200 nm/min.

2.4 *Temperature Measurement during NIR Radiation of SWNTs*

For *ex vitro* experiments, SWNT solutions (nanotube concentration of 3.5 μg/mL) were irradiated by the 980-nm laser at 1 W/cm^2. Temperature was measured in 10-s intervals with a thermocouple placed inside the solution for a total of 2 min. The thermocouple was placed outside the path of the laser beam to avoid direct exposure of the thermocouple to the laser light. For *in vivo* measurement, tumors with SWNTs were irradiated by the 980-nm laser at 1 W/cm^2. Surface temperatures of the tumors were measured in 30-s intervals with an infrared thermal camera (A40, FLIR, Boston, MA) for a total of 5 min. All the experiments were conducted at room temperature.

2.5 *Cell culture*

Murine mammary tumor line EMT6 cells were cultured in RPMI 1640 (GIBCO) supplemented with 15% fetal calf serum (FCS), penicillin (100 units/mL), and streptomycin (100 μg/mL) in 5% CO^2 and 95% air at 37 °C in a humidified incubator.

2.6 *SWNTs Functionalized by Various Phospholipids*

Solutions of SWNTs were functionalized with one or two phospholipid-poly (ethyleneglycol) PL-PEG molecules, PL-PEG-FA, or PL-PEG-FITC, following the procedures described by Kam et al.[9]

2.7 *FR+ Cells and FR– Cells*

EMT6 cells were cultured in FA-free RPMI-1640 medium (GIBCO). It is known that the FA-starved cells overexpress FRs on the cell surfaces. EMT6 cells were passaged for at least four rounds in the FA-free medium before use to ensure overexpression of FR on the surface of the cells (FR+ cells). FR− cells were harvested by culturing them in RPMI 1640 with abundant FA to give few available free FRs on the cell surfaces.[9]

2.8 *Tumor Model*

EMT6 cells (2×10^6) in a 100-μl solution were injected into the flank region in female Balb/c mice. Animals were used in experiments on days 7 to 10 after the inoculation of cells, when tumors were 5 to 7 mm in diameter.

2.9 *Laser Irradiation of Tumor Cells in Tissue Culture*

Cells (1×10^4 per well) growing in 35-mm Petri dishes were incubated with FA-SWNT suspension for 2 h, rinsed with phosphate buffered saline (PBS), and exposed to light at a fluence of 60 to 120 J/cm^2 (0.5 to 1 W/cm^2 for 2 min). The light source was a 980-nm semiconductor laser.

2.10 *Laser Irradiation of Mouse Tumors*

SWNT or FA-SWNT was injected directly into the center of each tumor at a dose of 1 mg/kg, 6 h before illumination with the 980-nm light (day 7 after inoculation with tumor cells). The light was delivered to the tumors on day 8 after tumor cell inoculation using a fiber optic delivery system. The power density at the illumination area, which encompassed the tumor and 0.5 to 1 cm of the surrounding skin, was 1 W/cm^2. The total light dose delivered to each tumor was 300 J/cm^2. During the laser irradiation, mice were anesthetized with an intraperitoneal injection of pentobarbital sodium and were restrained in a specially designed holder.

2.11 *Confocal Microscopy*

The cells were imaged by a commercial laser scanning microscope (LSM 510/ConfoCor 2) combination system (Zeiss, Jena, Germany) equipped with a Plan-Neofluar 40×/1.3 NA oil differential interference contrast microscope (DIC) objective. FITC excited at 488 nm with an Ar-ion laser (reflected by a HFT 488-nm beamsplitter HFT) and the fluorescence emission was recorded through a 500 to 550-nm infrared bandpass filter.

FITC fluorescence *in vivo* was measured on the stage of a stereo microscope (Lumar V12, Zeiss, Jena, Germany) with a hydrargyrum lamp (HBO100) as the light source. Six hours after the SWNT-FITC or FA-SWNT-FITC injection, the *mice were anesthetized with pentobarbital sodium and were restrained in a specially designed holder* for imaging analysis with a fluorescence stereo microscope. The light beam through a 470/40 nm bandpass filter was used to excite the fluorescent probes. The fluorescent emission was recorded through the 525/50-nm bandpass channel.

2.12 *Determination of Cell Cytotoxicity*

Cell cytotoxicity assay was performed with a colorimetric tetrazolium salt-based assay. To determine the cytotoxicity of SWNTs, tumor cells (1×10^3 per well) were cultured in a 96-well microplate for 24 h and then incubated with SWNTs of different concentrations for 12 h, rinsed with PBS, and incubated for another 72 h in complete medium. To detect photothermal cytotoxicity, tumor cells were incubated with FA-SWNT incubation for 2 h, followed by irradiation of the 980-nm laser at a fluence of 60 to 120 J/cm^2

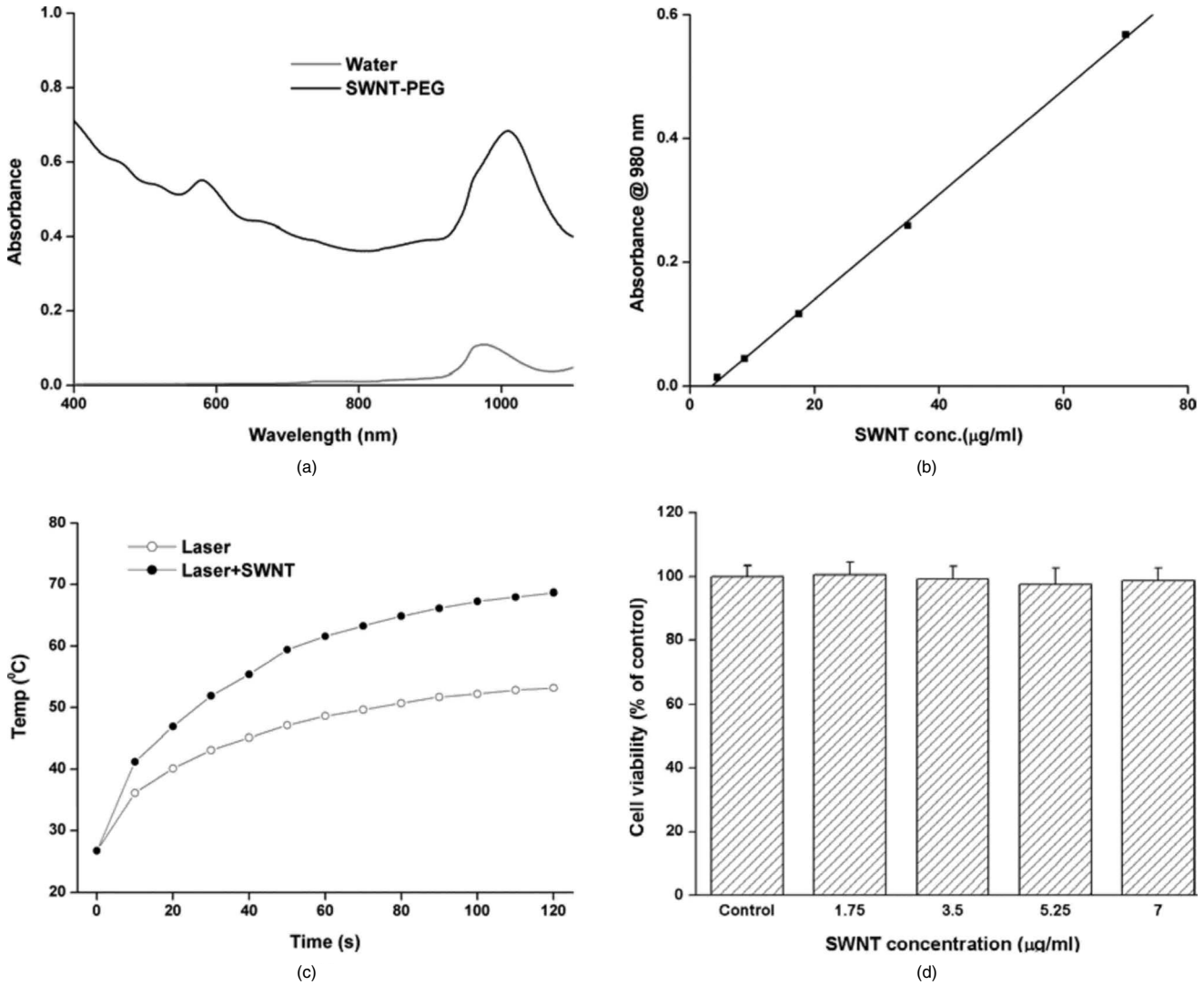

Fig. 1 Absorption spectra of CoMoCAT® single-walled carbon nanotubes solubilized in PEG. (a) UV-vis-NIR absorption spectra of the SWNTs suspension and water. (b) Absorbance of SWNT suspension of different concentrations at 980 nm (optical path=0.5 cm). The solid line is a linear fit. (c) Temperature measurements of an *ex vitro* control experiment using a SWNT solution (3.5 μg/mL) and water during irradiation by a 980-nm laser at 1 W/cm^2 for 2 min at room temperature. The results demonstrated the enhanced laser energy absorption by the SWNTs. (d) Cytotoxicity of SWNTs. Cells were incubated in the SWNT solution of different concentrations (1.75 μg/mL to 7 μg/mL) for 12 h, then washed and incubated in complete medium for 72 h before assessing cell viability. Cells not incubated with SWNTs were used as control. Bars (means+SD, n=4).

(0.5 to 1 W/cm^2 for 2 min). Cell cytotoxicity was assessed 12 h after the laser irradiation with CCK8. OD450, the absorbance value at 450 nm, was read with a 96-well plate reader (INFINITE M200, Tecan, Switzerland) to determine the viability of the cells.

2.13 *TUNEL Staining*

Individual tumors were obtained 3 h after laser treatment and were placed immediately in Tris-buffered zinc fixative [0.1 M Tris HCl buffer (pH 7.4) containing 3.2 mM calcium acetate, 22.8 mM zinc acetate, and 36.7 mM zinc chloride] for 6 to 18 h, transferred to 70% ethanol, dehydrated, and embedded in paraffin. Several cryostat sections, 10-μm thick, were cut from each tumor. DNA fragmentation of some tumor samples was detected by the terminal deoxynucleotide transferase-based, *in situ* cell death detection kit (TUNEL) according to the manufacturer's instructions. Biotinylated nucleotides incorporated into the DNA fragments were detected using a streptavidin-fluoresceine conjugate, which was excited with the 488-nm line of an Ar laser. Fluorescence was recorded using a 500 to 550-nm bandpass filter.

3 Results

3.1 *Absorption of Single-Walled Carbon Nanotubes Solubilized in PEG*

A stable SWNT-PEG suspension was obtained after the final centrifugation of the solution. The NIR absorption spectra of SWNT-PEG exhibited a strong band at approximately 980 nm, significantly higher than the water absorption in the same region [Fig. 1(a) and 1(b)], which is typical for CoMoCAT® samples.[10] To detect the effects of 980-nm opti-

cal excitation of SWNTs, we carried out a control experiment by radiating an aqueous solution of SWNTs *ex vitro*. We observed that irradiation of a SWNT solution (nanotube concentration of 3.5 μg/mL) by a 1-W/cm^2 (980-nm) laser for 2 min caused its temperature to elevate up to about 70 °C. However, the aqueous solution without SWNTs caused a temperature elevation to 55 °C [Fig. 1(c)]. These findings clearly demonstrat the enhanced absorption of the 980-nm light by the SWNTs.

3.2 *Cytotoxicity of Single-Walled Carbon Nanotubes Solubilized in PEG*

We investigated the cytotoxic effects of SWNTs using EMT6 tumor cells with CCK8 assay. EMT6 cells were cultured for 12 h with SWNTs of different concentrations (from 1.75 μg/mL to 7.5 μg/mL), washed, and then incubated for another 72 h in complete medium before detection. No cytotoxicity was observed, as shown in Fig. 1(d).

3.3 *Selective Targeting of Cancer Cells by FA-SWNT*

We use folate to determine whether SWNTs could be selectively internalized into cancer cells with specific tumor markers. To exploit this system, we obtained highly water-soluble individualized SWNTs noncovalently functionalized by PL-PEG-FA [Fig. 2(a)].[9] The FR-positive EMT6 cells (FR+ cells) with overexpressed FRs on the cell surfaces and the FR− cells without surface FRs were used (see Sec 2). Both FR+ and FR− cells were exposed to FA-SWNT for 2 h, washed, and then irradiated by a 980-nm laser (0.5 W/cm^2) for 2 min. After the irradiation, extensive cell death was observed in the FR+ cells, evidenced by drastic cell morphology changes [Fig. 2(b), upper panel], whereas the FR− cells remained intact [Fig. 2(b), lower panel]. These results show that FR+ cancer cells could selectively internalize FA-SWNT and could be selectively destroyed by irradiation of the 980-nm laser light.

3.4 *Laser Treatment of Tumor Cells with Different Concentrations of FA-SWNT—In Vitro Results*

We used CCK 8 assay investigate the effects of SWNTs on tumor cells during laser treatment. The tumor cells were incubated with FA-SWNT solution for 2 h, followed by irradiation with a 980-nm laser. The tumor cytotoxicity depended on both the SWNT concentration and the laser dose [Fig. 3(a)]. At a fluence of 60 J/cm^2, tumor cells treated by the laser without the presence of FA-SWNT remained essentially intact, while noticeable photothermal cellular cytotoxicity was observed with the presence of FA-SWNT. With a higher fluence (120 J/cm^2), the laser energy alone resulted in a marked cytotoxicity (37%). However, FA-SWNT significantly enhanced the photocytotoxicity. The FA-SWNT at 1.75 μg/mL and 3.5 μg/mL yielded cytotoxicity rates of 60% and 85% at 120 J/cm^2, as shown in Fig. 3(a). Figure 3(b) shows the effective destruction of tumor cells using laser irradiation (120 J/cm^2) with and without FA-SWNT (at a dose of 3.5 μg/mL). Apparently, both the FA-SWNT concentration and the laser dose are controlling factors for thermally induced cytotoxicity.

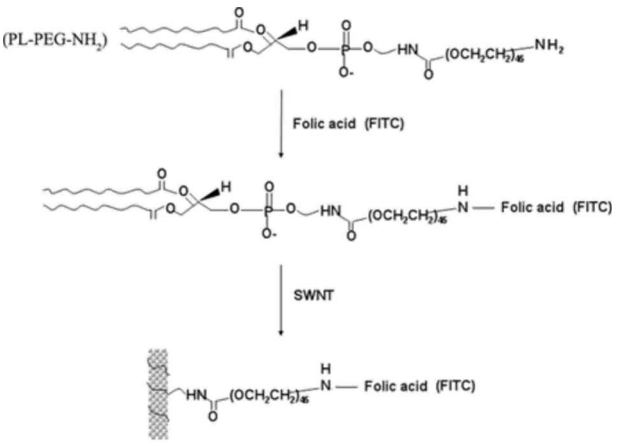

(a)

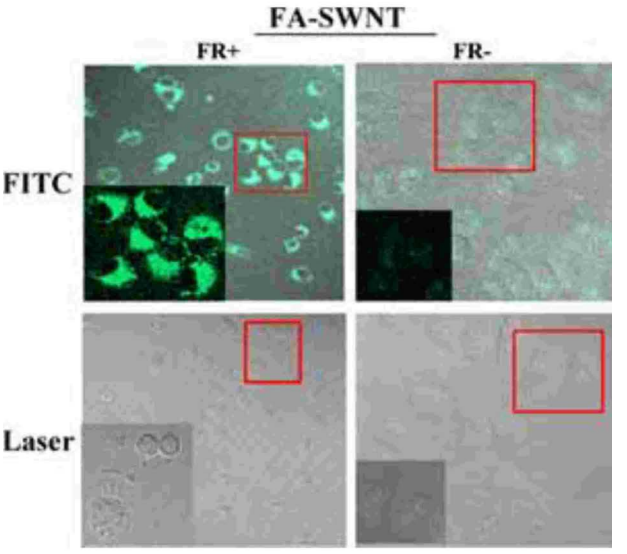

(b)

Fig. 2 Selective targeting and killing of cancer cells. (a) Chemical structure of PL-PEG-FA and PL-PEG-FITC synthesized by conjugating PL-PEG-NH$_2$ with FA or FITC, respectively, for solubilizing individual SWNTs. (b) Upper panel: Confocal images of EMT6 cells of FR+ or FR− after incubation in a solution of SWNTs with two cargoes (PL-PEG-FA and PL-PEG-FITC). The strong green FITC fluorescence inside the FR+ cells confirms the SWNT uptake by FA and FITC cargoes. The small amount of green fluorescence inside the FR− cells, confirmed the lack of SWNT uptake by FA and FITC cargoes (×40). (Inset) High-magnification images show the details of fluorescence in the cells. Lower panel: Images of dead FR+ cells with rounded cell morphology and unharmed FR− cells after irradiation (980-nm laser radiation at 0.5 W/cm^2 for 2 min). (Inset) High-magnification images show the details of the dead cells (FR+) and the live cells (FR−). (Color online only.)

3.5 *Laser Treatment of Mouse Tumors with FA-SWNT—In Vivo Results*

We used the mammary tumor model with EMT6 cells in the female Balb/c mice to investigate the *in vivo* effects of FA-SWNT. The mouse tumors with or without FA-SWNT were treated by the 980-nm laser. To determine the effects of NIR optical excitation of SWNTs inside tumors, we measured the temperature on the tumor surface during the irradiation by the 980-nm laser with an infrared thermal camera. In one experi-

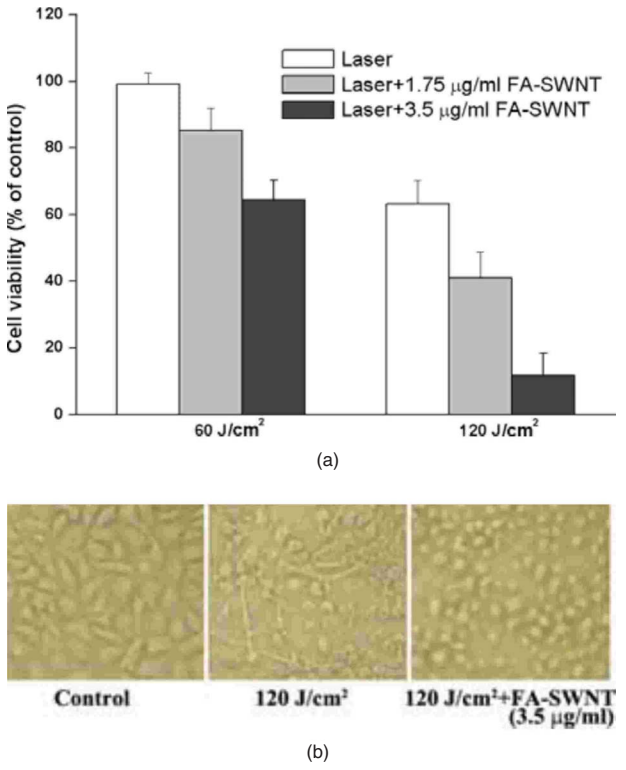

Fig. 3 Viability of tumor cells under different treatments. (a) Cells tumor cells treated with laser only or with laser-FA-SWNT. The treated cells were incubated in complete medium for 12 h before assessing cell viability. Cells without treatment were used as control. Bars (means+SD, n=4). (b) Optical images of tumor cells under different treatments as indicated.

mental mouse, irradiation of tumors with a power density of 1 W/cm^2 with FA-SWNT (1 mg/kg) for 5 min caused a surface temperature elevation of 63 °C [Fig. 4(a)]. Without FA-SWNT, the tumor irradiated at the same light dose caused a surface temperature elevation of 54 °C [Fig. 4(a)]. Experiments with other animals yielded similar results. These findings clearly show that FA-SWNT could effectively enhance the tumor photothermal therapy.

To investigate the SWNT distribution in tumors, we directly injected SWNT-FITC or FA-SWNT-FITC solution into the tumors, and the target tumors were observed with a fluorescence stereo microscope 6 h after the injection. The fluorescence of FA-SWNT was detected inside the tumors, but not in the normal tissue around the tumors [Fig. 4(b)]. However, the fluorescence of SWNT was detected in both the injected tumors and in surrounding normal tissue [Fig. 4(b)]. This indicates that the FA-SWNT has a greater higher affinity with tumor cells due to the tumor-specific antibodies, while SWNT alone could easily reach the surrounding tissue through intracellular diffusion.

To investigate the therapy effect of SWNT on tumors during laser treatment, we examined tissue sections from different samples by TUNEL staining. The tumors were directly injected with SWNT or FA-SWNT solution for 6 h, followed by irradiation with a 980-nm laser (1 W/cm^2 for 5 min). The tissue sections were obtained 3 h after treatment. TUNEL staining showed morphologically the treatment-induced cell death at different levels under different treatments. Tumors treated by the laser alone resulted in a marked cell death rate (56%), while a more significant cell death rate was observed with the presence of SWNT (78%) and FA-SWNT (88%), as shown in Figs. 4(c) and 4(d).

For the tissue section selected from normal tissue within the laser beam but about 0.5 cm away from the tumor, laser energy alone resulted in a low cell death rate (16%), as shown in Fig. 4(e), with SWNT enhancement, the cell death rate of normal tissue around the tumor was about 36%. However, the FA-SWNT administered to the mouse showed no impact on the normal tissue around the tumors with a cell death rate of 17.5%, similar to that of laser-only treatment, as shown in Figs. 4(c) and 4(e). These results clearly indicate that FA-SWNT could specifically target the tumor cells and enhance thermal damages to the target cells while not affecting normal tissues around the tumor.

4 Discussion

From a clinical perspective, it is important that mammalian cancer cells generally are more sensitive to heat-induced damage and apoptosis than normal cells.[24] SWNTs have a high optical absorbance in the NIR region,[9,16] where biological tissues are highly transparent.[18,19] CoMoCAT® nanotubes were used in this study because they exhibit a sharp absorption band at around 980 nm [Fig. 1(a)].[10] It is clear from our data that SWNTs released substantial heat after exposure to 980-nm laser irradiation *in vitro*, increasing the surrounding temperature [Fig. 1(c)]. This advantage could be used in selective photothermal therapy to assure lethal thermal injury to malignant cells while sparing normal cells.

Many solid tumors, including breast, lung, endometrium, cervix, ovary, and renal carcinoma cells, overexpress FRs on the cell cytoplasm membrane.[25,26] We combined SWNTs with specific ligands for recognizing and targeting tumor cells. Targeting FRs on the cell surface allows SWNTs to facilitate cellular internalization of folate-containing species by receptor-mediated endocytosis[27] which is more selective of tumor cells than SWNTs alone that enter cells through phagocytosis or endocytosis and through passive diffusion across lipid bilayers.[14,28,29] To exploit this system, we developed highly water-soluble, individualized SWNTs that were noncovalently functionalized by PL-PEG-FA [Fig. 2(a)]. Our results show that FA-SWNT could be selectively internalized into FR+ cancer cells, allowing selective destruction of FR+ cells under 980-nm light irradiation, without internalization into and destruction of FR− cells [Fig. 2(b)]. The former was a result of selective binding of FA-functionalized SWNTs and FRs on FR+ cell surfaces and receptor-mediated endocytosis, the latter was caused by the lack of available FRs on the FR− cells.[9]

Our results also showed that both the FA-SWNT concentration and the laser dose are controlling factors for thermally induced cytotoxicity [Fig. 3(a)]. Compared to laser irradiation alone, FA-SWNT significantly enhanced the photocytotoxicity [Figs. 3(a) and 3(b)]. These results indicated that SWNTs conjugated to folate could be used as a selective and efficient photothermal agent for cancer therapy with a 980-nm laser.

Our *in vivo* data clearly showed that as an intracellular target molecule, the FA-SWNTs released substantial heat after

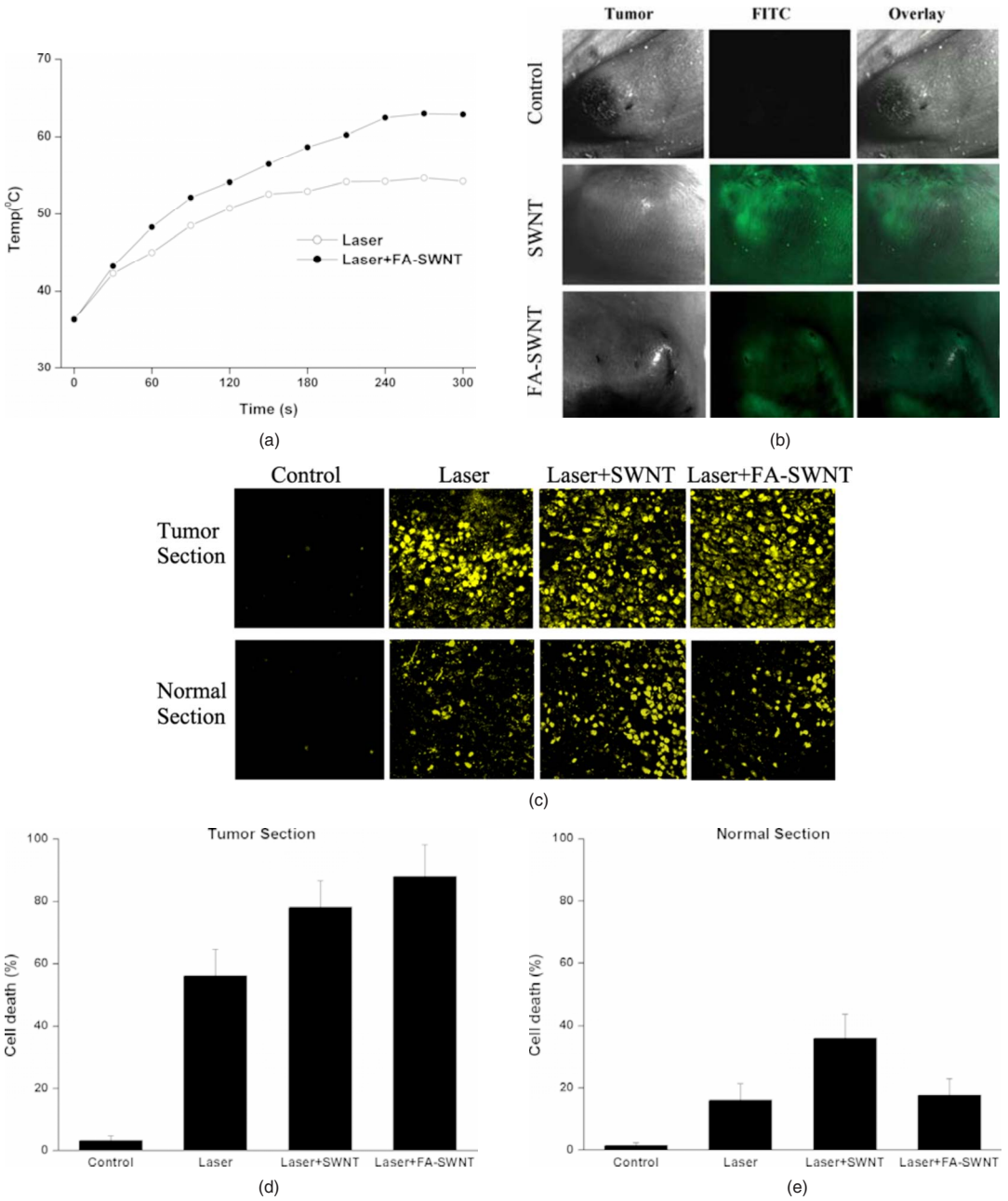

Fig. 4 Laser treatment induced cell death *in vivo*. (a) Temperature on the surface of a mouse tumor during irradiation by the 980-nm laser at 1 W/cm^2 for 5 min with and without FA-SWNT (1 mg/kg). This result clearly demonstrated the selective thermal effect caused by SWNT absorption of 980-nm light in the tumor. (b) Fluorescent emissions of FITC from a mouse tumor sample and normal tissue around the tumor, 6 h after injection, observed with a fluorescence stereo microscope. The normal tissue surrounding the tumor injected with SWNT-FITC shows more intense fluorescent emission than that surrounding the tumor injected with FA-SWNT-FITC. The control sample was injected with PBS. These results indicated that FA-SWNT has higher tumor selectivity than SWNT. (c) Images of tumor tissue (upper panel) and normal tissue (lower panel) sections after different treatments. TUNEL staining analysis of tissue sections from a mouse was performed 3 h after treatment. Samples were selected from the tumor and the normal tissue within the laser beam but 0.5 cm away from the tumor. This result clearly demonstrated that FA-SWNT enhanced the thermal damages of the tumor while contributing limited damage to the normal tissue around the tumors. (d) Cell death rates of the tumor section, after different treatments (100 cells/group ×5). (e) Cell death rates of the normal section after different treatments (100 cells/group ×5).

exposure to a 980-nm laser irradiation [Fig. 4(a)]. Furthermore, the FA-SWNTs showed high selectivity to bind to the tumor cells [Fig. 4(b)]. The TUNEL staining of tumor tissue sections clearly showed that either SWNT or FA-SWNT noticeably enhanced the photocytotoxicity compared to laser irradiation alone [Figs. 4(c) and 4(d)]. Compared to laser-SWNT treatment, laser-FA-SWNT treatment induced high levels of tumor destruction [Figs. 4(c) and 4(d)]—the result of a higher concentration of FA-SWNT selectively bound to the tumor tissue.

The TUNEL staining of normal tissue sections 0.5 cm away from the tumors showed that the laser-FA-SWNT treat-

ment yielded a noticeably lower rate of cell death (17.5%) in the normal tissue compared with the laser-SWNT treatment (36%), as shown in Figs. 4(c) and 4(e). This difference was caused by the fact that SWNTs by themselves could be internalized into normal tissue cells around the tumor tissue, which enhanced the normal cell cytotoxicity, while FA-SWNT would be selectively bound to the surface of tumor cells, which reduced the normal cell cytotoxicity.

In summary, FA-SWNT effectively enhanced the photothermal destruction of tumor cells and noticeably protected the photothermal destruction of normal cells. Thus, SWNTs combined with suitable tumor markers can be used as novel nanomaterials for targeted cancer photothermal therapy. Our study demonstrated such potential based on the folate conjugation. Further studies are needed to investigate the effectiveness of FA-SWNT and SWNTs conjugated with other biomarkers in selective photothermal therapy for cancer treatment.

Acknowledgements

This research was supported in part by the National Natural Science Foundation of China (30470494, 30627003), the Natural Science Foundation of Guangdong Province (7117865), the U.S. National Institutes of Health (P20 RR016478 from the IDeA Network of Biomedical Research Excellence (INBRE) Program of the National Center for Research Resources), and the U.S. Department of Energy-Basic Energy Sciences (DE-FG03-02ER15345 and DE-FG02-06ER64239).

References

1. Z. Amin, J. J. Donald, A. Masters, R. Kant, A. C. Steger, S. G. Bown, and W. R. Lees, "Hepatic metastases: interstitial laser photocoagulationwith real-time US monitoring and dynamic CT evaluation of treatment," *Radiology* **187**, 339–347 (1993).
2. C. P. Nolsoe, S. Torp-Pedersen, F. Burcharth, T. Horn, S. Pedersen, N. E. Christensen, E. S. Olldag, P. H. Andersen, S. Karstrup, and T. Lorentzen, "Interstitial hyperthermia of colorectal liver metastases with a US-guided Nd-YAG laser with a diffuser tip: a pilot clinical study,"*Radiology* **187**, 333–337 (1993).
3. T. J. Vogl, M. G. Mack, P. K. Müller, R. Straub, K. Engelmann, and K. Eichler, "Intervention MR imaging: percutaneous abdominal and skeletal biopsy and drainages of the abdomen," *Eur. Radiol.* **9**, 1479–1487 (1999).
4. W. R. Chen, R. L. Adams, K. E. Bartels, and R. E. Nordquist, "Photothermal effects on murine mammary tumors using indocyanine green and an 808-nm diode laser: an in vivo efficacy study," *Cancer Lett.* **94**, 125–131 (1995).
5. W. R. Chen, R. L. Adams, A. K. Higgins, K. E. Bartels, and R. E. Nordquist, "Photothermal effects on murine mammary tumors using indocyanine green and an 808-nm diode laser: an in vivo efficacy study," *Cancer Lett.* **98**, 169–173 (1996).
6. C. Loo, A. Lowery, N. Halas, and J. West, R. Drezek, "Immunotargeted nanoshells for integrated cancer imaging and therapy," *Nano Lett.* **5**, 709–711 (2005).
7. L. R. Hirsch, R. J. Stafford, J. A. Bankson, S. R. Sershen, B. Rivera, R. E. Rrice, J. D. Hazle, N. J. Halas, and J. L. West, "Nanoshell-mediated near-infrared thermal therapy of tumors under magnetic resonance guidance," *Proc. Natl. Acad. Sci. U.S.A.* **100**, 13549–13554 (2003).
8. D. P. O'Neal, L. R. Hirsch, N. J. Halas, J. D. Paynea, and J. L. West, "Photo-thermal tumor ablation in mice using near infrared-absorbing nanoparticles," *Cancer Lett.* **209**, 171–176 (2004).
9. N. W. S. Kam, M. J. O'Connell, J. A. Wisdom, and H. Dai, "Carbon nanotubes as multifunctional biological transporters and near-infrared agents for selective cancer cell destruction," *Proc. Natl. Acad. Sci. U.S.A.* **102**, 11600–11605 (2005).
10. S. M. Bachilo, L. Balzano, J. E. Herrera, F. Pompeo, D. E. Resasco, and R. B. Weisman, "Narrow (n,m)-distribution of single-walled carbon nanotubes grown using a solid supported catalyst," *J. Am. Chem. Soc.* **125**, 11186–11187 (2003).
11. R. J. Chen, S. Bangsaruntip, K. A. Drouvalakis, N. W. Kam, M. Shim, Y. Li, W. Kim, P. J. Utz, and H. Dai, "Noncovalent functionalization of carbon nanotubes for highly specific electronic biosensors," *Proc. Natl. Acad. Sci. U.S.A.* **100**, 4984–4989 (2003).
12. J. J. Gooding, R. Wibowo, J. Liu, W. Yang, D. Losic, S. Orbons, F. J. Mearns, J. G. Shapter, and D. B. Hibbert, "Protein electrochemistry using aligned carbon nanotube arrays," *J. Am. Chem. Soc.* **125**, 9006–9007 (2003).
13. R. H. Baughman and A. A. Zakhidov, "Carbon nanotube actuators," *Science* **284**, 1340–1344 (1999).
14. D. Pantarotto, J. P. Briand, M. Prato, and A. Bianco, "Translocation of bioactive peptides across cell membranes by carbon nanotubes," *Chem. Commun. (Cambridge)* **1**, 16–17 (2004).
15. N. W. S. Kam, T. C. Jessop, P. A. Wender, and H. Dai, "Nanotube molecular transporters: internalization of carbon nanotube-protein conjugates into mammalian Cells," *J. Am. Chem. Soc.* **126**, 8650–8651 (2004).
16. M. J. O'Connell, S. M. Bachilo, C. B. Huffman, V. C. Moore, M. S. Strano, E. H. Haroz, K. L. Rialon, P. J. Boul, W. H. Noon, and C. Kittrell, "Band gap fluorescence from individual single-walled carbon nanotubes," *Science* **297**, 593–596 (2002).
17. C. J. Gannon, P. Cherukuri, B. I. Yakobson, L. Cognet, J. S. Kanzius, C. Kittrell, R. B. Weisman, M. Pasquali, H. K. Schmidt, R. E. Smalley, and S. A. Curley, "Carbon nanotube-enhanced thermal destruction of cancer cells in a noninvasive radiofrequency field," *Cancer* **110**, 2654–2665 (2007).
18. K. König, "Multiphoton microscopy in life sciences," *J. Microsc.* **200**, 83–104 (2000).
19. R. Weisslder, "A clearer vision for in vivo imaging," *Nat. Biotechnol.* **19**, 316–317 (2001).
20. B. Kitiyanan, W. E. Alvarez, J. H. Harwell, and D. E. Resasco, "Controlled production of single-wall carbon nanotubes by catalytic decomposition of CO on bimetallic Co–Mo catalysts," *Chem. Phys. Lett.* **317**, 497–503 (2000).
21. X. Huang, I. H. EI-Sayed, W. Qian, and M. A. EI-Sayed, "Cancer cell imaging and photothermal therapy in the near-infrared region by using gold nanorods," *J. Am. Chem. Soc.* **128**, 2115–2120 (2006).
22. I. H. EI-Sayed, X. Huang, and M. A. EI-Sayed, "Selective laser photo-thermal therapy of epithelial carcinoma using anti-EGFR antibody conjugated gold nanoparticles," *Cancer Lett.* **239**, 129–135 (2006).
23. Z. Liu, W. Cai, L. He, N. Nakayama, K. Chen, X. Sun, X. Chen, and H. Dai, "In vivo biodistribution and highly efficient tumour targeting of carbon nanotubes in mice," *Nat. Nanotechnol.* **2**, 47–52 (2007).
24. H. H. Kampinga, "Cell biological effects of hyperthermia alone or combined with radiation or drugs: a short introduction to newcomers in the field," *Int. J. Hyperthermia* **22**, 191–196 (2006).
25. S. D. Weitman, A. G. Weinberg, L. R. Coney, V. R. Zurawski, D. S. Jennings, and B. A. Kamen, "Cellular localization of the folate receptor: potential role in drug toxicity and folate homeostasis," *Cancer Res.* **52**, 6708–6711 (1992).
26. M. Bagnoli, S. Canevari, and M. Figini, "A step further in understanding the biology of the folate recep tor in ovarian carcinoma," *Gynecol. Oncol.* **88**, S140–144 (2003).
27. Y. J. Lu, E. Sega, C. P. Leamon, and P. S. Low, "Eolate receptor-targeted immunotherapy of cancer: mechanism and therapeutic potential," *Adv. Drug Delivery Rev.* **56**, 1161–1176 (2004).
28. N. W. S. Kam, Z. Liu, and H. Dai, "Carbon nanotubes as intracellular transporters for proteins and DNA: An investigation of the uptake mechanism and pathway," *Angew. Chem., Int. Ed.* **44**, 1–6 (2005).
29. A. E. Porter, M. Gass, K. Muller, J. N. Skepper, P. A. Midgley, and M. Welland, "Direct imaging of single-walled carbon nanotubes in cells," *Comput. Theor. Polym. Sci.* **2**, 713–717 (2007).